Journal of Alloys and Compounds 509 (2011) 1729–1733

Contents lists available at ScienceDirect

Journal of Alloys and Compounds

journal homepage: www.elsevier.com/locate/jallcom

Enhanced optical modulation due to SPR in gold nanoparticles embedded WO_3 thin films

P.M. Kadam[a], N.L. Tarwal[e], P.S. Shinde[e], S.S. Mali[e], R.S. Patil[b], A.K. Bhosale[c], H.P. Deshmukh[d], P.S. Patil[e,*]

[a] Department of Electronics, Smt. Kasturbai Walchand College, Sangli 416416, India
[b] Department of Physics, The New College, Kolhapur 416012, India
[c] Department of Physics, Raje Ramrao Mahavidhyalaya, Jath 416005, India
[d] Department of Physics, Y.M. College, Pune, India
[e] Thin Film Materials Laboratory, Department of Physics, Shivaji University, Kolhapur 416004, India

ARTICLE INFO

Article history:
Received 5 April 2010
Received in revised form 6 October 2010
Accepted 7 October 2010
Available online 15 October 2010

Keywords:
WO_3
Thin film
PSPT
Optical modulation
SPR

ABSTRACT

Surface plasmon resonance (SPR) phenomenon of metal–dielectric composite thin films formed by embedding the noble metal nanoparticles in a dielectric matrix offers a high degree of flexibility and enables many applications such as surface enhanced spectroscopes, numerous biological and chemical sensing fields. A remarkable enhancement in optical modulation after embedding the gold nanoparticles in a reticulated mesh like matrix of WO_3 thin films was observed. WO_3 films were prepared onto the conducting ITO coated glass substrates by a novel pulsed spray pyrolysis technique (PSPT). A reticulated mesh like morphology of WO_3 was achieved by optimizing the deposition parameters of PSPT and the gold nanoparticles were embedded in the WO_3 matrix by a drop casting method. Enhancements in electrochromic properties of WO_3 in terms of optical modulation (ΔOD), coloration efficiency (η) and response times (t_c and t_b) were attributed to the assistance of SPR in gold nanoparticles during coloration and electric field induced quenching of SPR during bleaching.

1. Introduction

Electrochromism is a reversible change in optical density leading to coloration and bleaching under the application of a small electric potential difference. Transition metal oxides such as WO_3, MoO_3, NiO, etc. exhibit electrochromism owing to their defect perovskite structure. The coloration and bleaching is attributed to intervalence charge transfer (reduction and oxidation) reactions due to intercalation and deintercalation of light positive ions like H^+, Li^+, Na^+, OH^- into the host lattice [1–6]. Electrochromic WO_3 thin films exhibit blue coloration upon insertion of Li^+ or H^+ ions and find potential applications as smart windows, energy savers, information displays, etc. [1,7]. An efficient electrochromic material for smart window application must have fast intercalation/deintercalation kinetics and large changes in optical density per unit inserted charge [8] along with good reversibility and stability. Insertion kinetics depends upon diffusion coefficient (D), which eventually depends on crystal structure and diffusion path determined by microstructure of the material [9].

Surface plasmon resonance (SPR) phenomena at the metal–dielectric interface have enabled a vast array of applications such as surface enhanced spectroscopes, and biological and chemical sensing, electrochromic windows [10,11]. The materials used for supporting surface plasmon waves must have free conduction band electrons capable of resonating with the incoming light at a suitable wavelength. Some of the metals that satisfy this requirement include Ag, Au, Ti, Cr, Cu, Al, and In. Among these, the metal nanoparticles (~50 nm) like Au and Ag are used to support SPR since other metals are either too reactive or too expensive or too susceptible to oxidation [12]. Au and Ag exhibit SPR as a result of interaction between electromagnetic radiation and loosely bound electrons to the metal surface. For example, gold nanoparticles of about 60 nm size show SPR absorption in red region imparting blue color to them [13]. Hence, embedding such nanoparticles into the WO_3 matrix could enhance its optical density change.

Bathe and Patil [14–16] investigated the reticulated mesh like morphology in pristine and doped WO_3 thin films deposited by pulsed spray pyrolysis technique (PSPT). Coloration efficiency of 34 cm^2/C is reported for pristine WO_3; however Nb and Ti doping is found to have detrimental effect on electrochromic performance. Use of SPR for gas sensing or electrochromic applications is rather a new subject and very few research articles can be seen

* Corresponding author. Tel.: +91 231 2609230; fax: +91 231 2691533.
E-mail address: psp_phy@unishivaji.ac.in (P.S. Patil).

0925-8388/$ – see front matter © 2010 Elsevier B.V. All rights reserved.
doi:10.1016/j.jallcom.2010.10.024

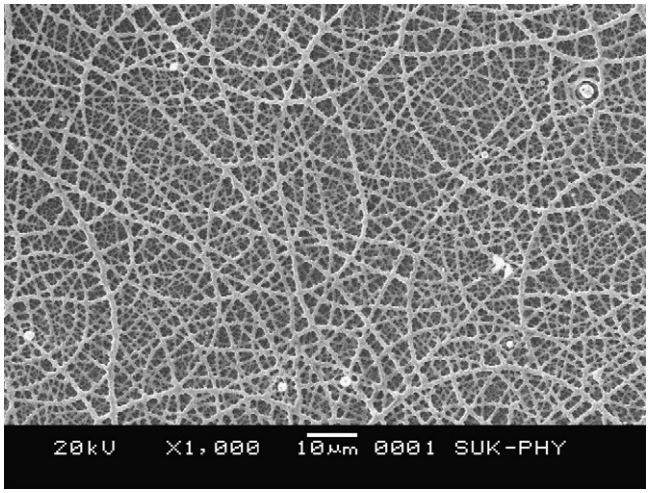

Fig. 1. SEM image of pure WO_3 thin film revealing reticulated mesh like morphology.

in the literature. Chen et al. [10] explored the SPR phenomenon in Au–WO_{3-x} films in view of their use for NO gas sensor. WO_3 nanorods modified by Au nanoparticles are found be useful for H_2 gas sensors that showed enhanced response and selectivity. Such nanorods degraded the organic impurities with high photocatalytic activity owing to increased absorption in the UV–vis region as compared to pure WO_3 [17]. More recently, Au nanocrystal-doped WO_3 sol–gel films exhibited improved electrochromic properties exhibiting 10 times faster coloration time than that of pure WO_3 [18]. Au nanoparticles can also have adverse effect on optical properties. RF sputtered Au–WO_3 electrodes showed reverse optical modulation than that of pure WO_3 electrode with respect to applied potential in 0.5 M H_2SO_4 [11,19]. Authors attributed this modification for dispersion of conducting Au nanophases in the WO_3.

In the present investigation, we have studied the effect of Au nanoparticles on the electrochromic properties of WO_3 films obtained from a novel PSPT. Au nanoparticles were successfully embedded into the reticulated matrix of WO_3 by a simple and facile drop casting method. The observed enhancement in optical modulation of WO_3 thin films is presumed to be due to the SPR assisted coloration phenomenon.

2. Experimental details

For deposition of WO_3 thin films, 20 ml of 50 mM ammonium tungstate precursor was sprayed onto the preheated tin doped indium oxide (ITO) coated glass substrates using PSPT [20]. The deposition temperature was maintained at 450 °C by keeping other parameters constant at their optimized values to yield a uniform, transparent and well adherent WO_3 film (films thickness ~250 nm). Gold nanoparticles were synthesized by a method reported elsewhere [21]. A quantity of 90 ml of 10 mM aqueous solution of chloroauric acid ($HAuCl_4$) was reduced by 10 ml of 1 mM aqueous solution of tryptophan (Aldrich Chemicals). Mild heating at 50 °C yielded stable gold nanoparticles in water. The solution containing tryptophan-reduced gold nanoparticles was subjected to ultra centrifugation and the resulting precipitate was washed with copious amount of deionized water to eliminate any uncoordinated tryptophan molecules. The average size of nanoparticles was estimated to be 60–70 nm. These gold nanoparticles were embedded into the matrix of WO_3 by a drop casting method using 4 and 8 drops of Toluene to produce the gold surface densities of 0.008 and 0.017 cc/cm^2, respectively and the respective samples were designated as Au-4 and Au-8. A pristine WO_3 sample without Au particles was designated as Au-0. All the three samples viz. Au-0, Au-4 and Au-8 were further subjected to various characterizations.

The surface morphology of the films was studied using scanning electron microscope (SEM) model JEOL-JSM-6360 equipped with energy dispersive x-ray analysis (EDAX). The film was also characterized using transmission electron microscope (TEM) to evidence the presence of Au nanoparticles. The transmittance spectra in colored and bleached states were recorded using a UV–vis–NIR spectrophotometer in the wavelength range of 350–850 nm. Electrochromical characterization was carried out using EG & G Make Versastat-II model PAR 362 controlled by M270 software. The electrochromic measurements were carried out using 0.5 M $LiClO_4$ in propylene carbonate electrolyte with a three electrode cell configuration consisting of WO_3 sample as working electrode, graphite as counter electrode and saturated calomel electrode (SCE) as a reference electrode.

3. Results and discussion

Fig. 1 shows SEM image for pure WO_3 thin film without gold nanoparticles (Au-0). The image clearly exhibits a reticulated mesh like morphology, which is very common for spray deposited WO_3 films [14,22]. Such morphology is more suitable for embedding nano-Au particles as well as for providing an easy pathway for diffusion of ions/electrons during intercalation and deintercalation processes. After embedding Au nanoparticles, the morphology of WO_3 remains unchanged as observed from SEM study. Hence, TEM is employed to get evidence for presence of Au nanoparticles into the WO_3 matrix. TEM can also be a good tool for revealing the particle size of the deposited nanostructures. Fig. 2 shows a TEM image of a WO_3 sample embedded with 0.008 cc/cm^2 nano-gold particles. It is observed that the size of the gold nanoparticles (NPs) varied from 10 to 60 nm. A careful observation of TEM image suggests that

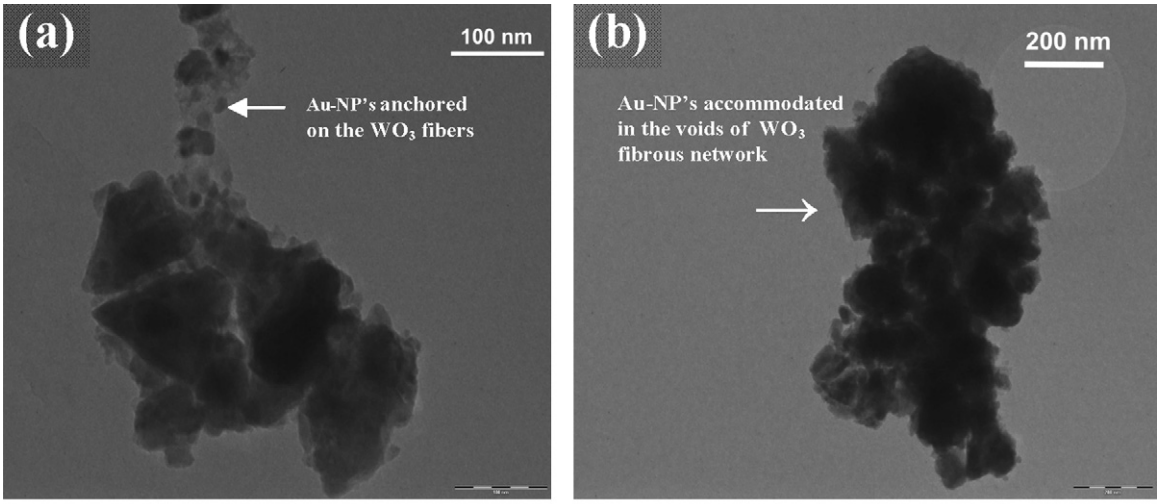

Fig. 2. TEM images for the Au–WO_3 thin films at different quantities of nano-Au particles anchored on WO_3; (a) Au-4 and (b) Au-8.

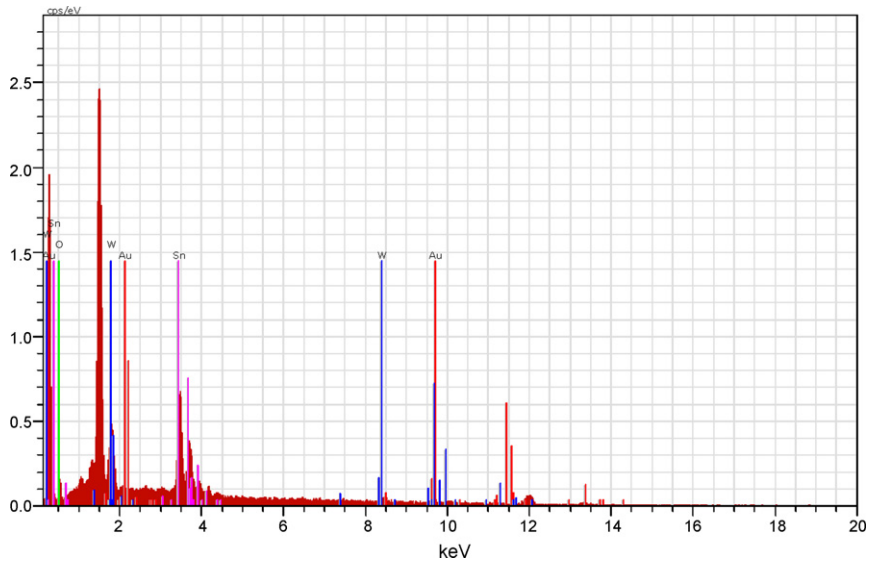

Fig. 3. EDAX spectrum of typical Au–WO_3 thin film (sample Au-8).

small-sized Au nanoparticles are anchored on WO_3 fibers and relatively larger ones are accommodated in the voids formed by the fibrous network. Thus, Au-NPs are embedded into the WO_3 matrix in an effective way. The loading of Au nanoparticles is also confirmed from EDAX spectrum. Fig. 3 shows a typical EDAX spectrum of Au-8 WO_3 thin film. After judicious selection of the samples, their electrochemical stability and electrochromic properties are examined.

Fig. 4 shows cyclic voltammograms (CVs) of the pure and Au-anchored WO_3 samples recorded at the scan rate of 50 mV/s in a 0.5 M $LiClO_4$ + PC electrolyte over the potential range from −0.5 to 0.8 V versus SCE. The nature of CV for pure WO_3 sample is as per expectation, which exhibited a characteristic cathodic spike and anodic peak. The originally transparent WO_3 sample undergoes cathodic reduction due to intercalation of Li^+ ions towards extreme cathodic potentials as a result of $\{WO_3 + Li^+ + e^- \rightarrow Li_xWO_3\}$ reaction and, eventually responsible for blue coloration. Upon anodic polarization, oxidation of sample takes place and Li^+ ions de-intercalate, to acquire a bleached transparent state as a result of $\{Li_xWO_3 \rightarrow WO_3 + Li^+ + e^-\}$ reaction. The ubiquitous intervalence charge transfer (IVCT) mechanism renders blue coloration to the WO_3 film [14]. The IVCT mechanism essentially remains same but the extent of (de)intercalated charges wane with the increment in the amount of Au-NPs embedded into the WO_3 matrix. This fact is resembled from comparison of CVs recorded for Au-0, Au-4 and Au-8 samples. CVs of Au-anchored WO_3 films comprised of less area under the curve as compared to pure WO_3. This suggests that the Au-NPs hinder the intercalation pathways as they occupy the void spaces of the WO_3 matrix by virtue of which the transport channels become inaccessible to the ions. With increase of Au-NPs causes further loss of ionic intercalation–deintercalation capability of the WO_3. Au-8 is the optimum quantity of the Au-NPs that can be embedded in the present study. To study the reaction kinetics of (de)intercalation processes chronoamperometry (CA) technique was used. Fig. 5 shows the CA curves revealing current–time response for pure and Au-anchored WO_3 samples in a 0.5 M $LiClO_4$ + PC electrolyte upon application of a step potential of ±0.5 V versus SCE for 10 s. In accordance with the theory [1], a well-known asymmetric behaviour is observed for all the WO_3

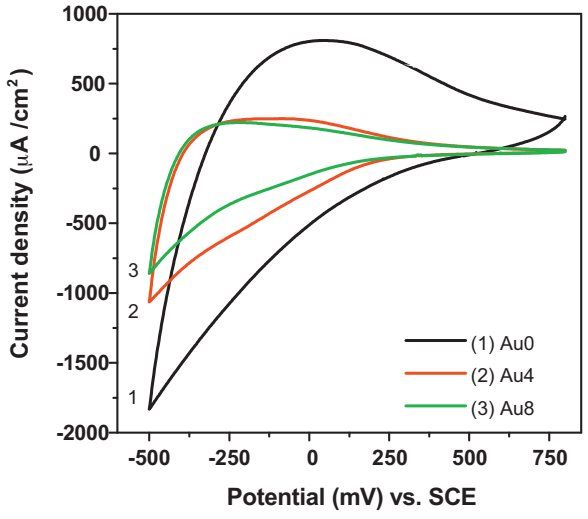

Fig. 4. Cyclic voltammograms of the WO_3 samples: (1) Au-0, (2) Au-4, and (3) Au-8, recorded at the scan rate of 50 mV/s in 0.5 M $LiClO_4$ + PC electrolyte over the potential range from −0.5 to 0.8 V versus SCE.

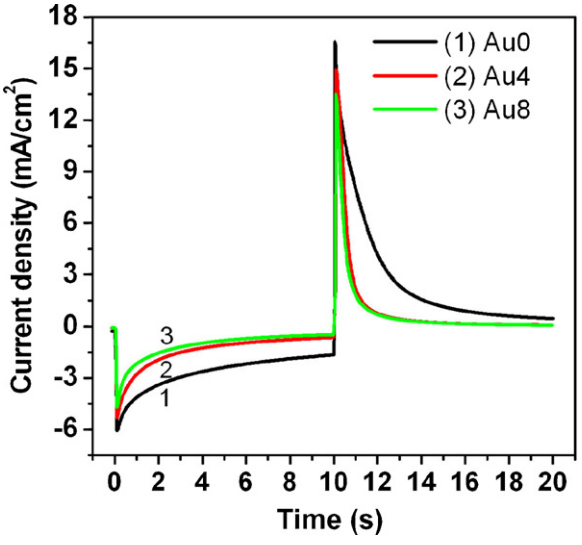

Fig. 5. Chronoamperometry curves of the WO_3 samples: (1) Au-0, (2) Au-4, and (3) Au-8, recorded in 0.5 M $LiClO_4$ + PC electrolyte upon application of step potential of ±0.5 V versus SCE for 10 s.

Table 1
Electrochromic parameters of the pure and Au-anchored WO_3 thin films.

Sample	Transmittance, T		Q_i (mC/cm^2)	Coloration efficiency, η (cm^2/C)	Response time (s)		Diffusion coefficient, D (cm^2/s)
	T_b	T_c			t_b	t_c	
Au-0	0.80	0.51	26	43	6.0	7.54	3.8×10^{-11}
Au-4	0.78	0.34	14	59	4.6	5.35	2.2×10^{-11}
Au-8	0.75	0.23	11	108	4.7	4.75	1.7×10^{-11}

samples, with cathodic current being smaller and anodic current being larger. This asymmetric behaviour suggests that the Au-4 and Au-8 samples do not impede kinetic process of ionic intercalation and deintercalation. Response time is one of the most important electrochromic parameters of a film concerning its practical applications. Response time for coloration (t_c) and bleaching (t_b) is the time required for the anodic/cathodic current to achieve a steady state level after the application of reactive voltages. The response times (t_c and t_b) of all the samples are determined from CA study. All the electrochromic parameters including response times for pure and Au-anchored WO_3 samples are listed in Table 1. It is seen that the response times t_c and t_b decreased considerably with Au incorporation from 7.54 to 4.75 and from 6 to 4.7, respectively. The t_c for Au-4 and Au-8 samples is almost half than that for pure Au-0 sample, suggesting faster response time upon Au incorporation. This may be due to the fact that the amount and extent of ions intercalated into the WO_3 matrix decreases (as studied from CV study) and hence relatively fewer ions take part in the reaction. Their transport becomes much faster due to additional conductivity imparted by Au-NPs to the WO_3. Hence coloration-bleaching kinetics is faster for Au-4 and Au-8 samples. Diffusion coefficient of Li^+ in pure and Au-anchored WO_3 samples is determined from CVs recorded at different scan rates. It can be determined from logarithmic graph of current versus time as described in our earlier article [23]. The diffusion coefficient decreases from 3.8×10^{-11} to 1.7×10^{-11} cm^2/s with incorporation of Au nanoparticles. The reduction in diffusion coefficient of Li^+ ion for Au-4 and Au-8 samples further confirms the fact that the extent of ionic intercalation wanes, complementing to the CV results. This result is in contrast to the literature [18] where D values increase from 1×10^{-8} to 5×10^{-8} cm^2/s with increasing content of Au nanoparticles in WO_3 thin films deposited by sol–gel technique. The magnitudes of 'D' in both the cases differ due to the different methods of fabrication. Sol–gel method facilitates thin film deposition at lower temperatures as compared to the PSPT. Hence PSPT grown samples are relatively more compact and adherent to the substrates.

Fig. 6 shows the transmittance spectra of thin films in their colored and bleached states. The coloration efficiency (η) was estimated using change in optical density (ΔOD) at $\lambda = 630$ nm and intercalated charge density (Q_i) by Eq. (1),

$$\eta = \frac{\Delta OD_{\lambda=630\,nm}}{Q_i} = \frac{\ln(T_b/T_c)}{q/A} \quad (1)$$

where T_b and T_c are the transmittance values of the film in its bleached and colored state, respectively. q is the charge and A is the active area of the film. High value of η for electrochromic film means that electrochromic device should have adequate optical regulation upon less intercalation of charges and causing a better stability and reproducibility of colored/bleached (c/b) cycles. The value of η increased from 42.7 cm^2/C for pure Au-0 to 108 cm^2/C for Au-8 sample. On the contrary, Naseri et al. reported decrease in η from 35 to 7 cm^2/C with incorporation of Au nanoparticles. Though, the amount of intercalated charges is subsequently reduced for Au-embedded films in our case, there is large increase in ΔOD and η. This implies the existence of an additional complementary mechanism that can be attributed to SPR in Au-NPs [13].

Enhancement in electrochromism of WO_3 thin films by incorporation of Au-NPs is studied by He et al. [24,25]. They have attributed this enhancement to the change in conductivity of the electrode, which increases the rate of electrochromic reaction and Schottky barrier formed at the WO_3/Au interface and surface effect of gold nanoparticles. However, on account of the observed decrement in cathodic peak current (Fig. 4), i.e. intercalated charge for embedded films, we propose that the SPR of gold nanoparticles assist the coloration process and the SPR quenching by high electrostatic field does not affect the bleaching process resulting in an enhanced optical modulation. The proposed mechanism is as follows:

(i) During coloration, the electrochromic intervalence charge transfer reaction

$$WO_3 + xLi^+ + xe^- \rightarrow Li_xW^{+6}_{1-x}W^{+5}_xO_3$$

gives rise to absorption in the near IR region thereby imparting a blue color to the film. At the same time, the SPR in Au-NPs cause photonic absorption in the red region, rendering blue color to the gold nanoparticles. Thus, both electrochromic and SPR are going hand in hand and subsequently boost the coloration process.

(ii) During bleaching, the electrochromic intervalence charge transfer reaction

$$Li_xW^{+6}_{1-x}W^{+5}_xO_3 \rightarrow WO_3 + xLi^+ + xe^-$$

provides deintercalation and bleaches the film. Due to high electric field of the order of 10^7 V/m generated around Au-NPs, the SPR phenomenon is quenched and hence does not affect the bleaching process.

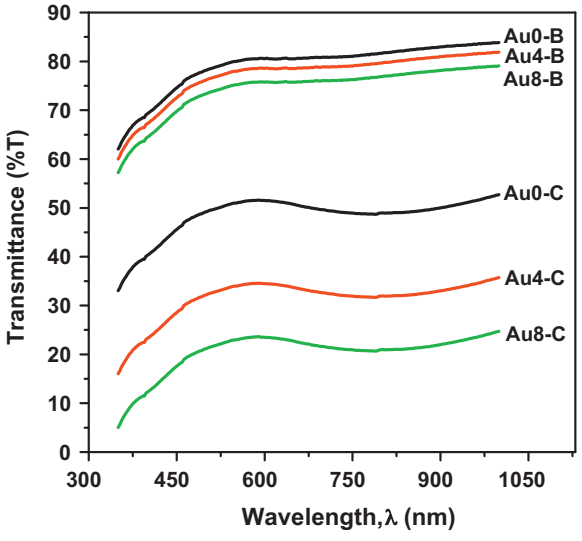

Fig. 6. Transmittance spectra for colored (C) and bleached (B) states of WO_3 samples: Au-0, Au-4, and Au-8.

This proposition however requires more detailed study to ascertain the aforementioned phenomena. This is our future work.

4. Conclusions

In conclusion, the SPR phenomenon by embedded gold nanoparticles can exclusively be used to enhance the optical modulation in an electrochromic host matrix like WO_3. The enhanced optical modulation at a lower level of intercalated charge increases the coloration efficiency and decreases the response times. The proposed mechanism of SPR assisted coloration and electric field induced SPR quenching during bleaching seems to be the working mechanisms of Au-NPs embedded spray pyrolyzed WO_3 with reticulated mesh like morphology.

Acknowledgements

Authors wish to acknowledge University Grants Commission (UGC), New Delhi and Department of Atomic Energy-Board of Research in Nuclear Sciences (DAE-BRNS), Mumbai, India for the financial assistance.

References

[1] C.G. Granqvist, Handbook of Inorganic Electrochromic Materials, Elsevier, Amsterdam, 1995.
[2] S.-H. Lee, H.M. Cheong, J.-G. Zhang, A. Mascarenhas, D.K. Benson, S.K. Deb, Appl. Phys. Lett. 74 (1999) 242.
[3] A.C. Sonavane, A.I. Inamdar, P.S. Shinde, H.P. Deshmukh, R.S. Patil, P.S. Patil, J. Alloys Compd. 489 (2010) 667.
[4] S.S. Kalagi, D.S. Dalavi, R.C. Pawar, N.L. Tarwal, S.S. Mali, P.S. Patil, J. Alloys Compd. 493 (2010) 335.
[5] M. Grätzel, Nature 409 (2001) 575.
[6] M. Wagemaker, A.P.M. Kentgens, F.M. Mulder, Nature 418 (2002) 397.
[7] C.G. Granqvist, in: J. Garcia-Martinez (Ed.), Nanotechnology for the Energy Challenge, Wiley-VCH Verlag GmbH & Co. KGaA, Weinheim, Germany, 2010.
[8] S.H. Lee, H.M. Cheong, C.E. Tracy, A. Mascarenhas, A.W. Czanderne, S.K. Deb, Appl. Phys. Lett. 75 (1999) 1547.
[9] S.H. Lee, H.M. Cheong, C.E. Tracy, A. Mascarenhas, J.R. Pitts, G. Jorgensen, S.K. Deb, Appl. Phys. Lett. 76 (2000) 3908.
[10] B. Chen, D. Yang, C.-W. Lin, Appl. Phys. A 97 (2009) 489.
[11] K.-W. Park, Electrochim. Acta 50 (2005) 4690.
[12] H. Deng, D. Yang, B. Chen, C.-W. Lin, Sens. Actuators, B 134 (2008) 502.
[13] C. Kumar (Ed.), Tissue, Cell and Organ Engineering, Wiley VHC, Weinheim, Germany, 2006.
[14] S.R. Bathe, P.S. Patil, Sol. Energy Mater. Sol. Cells 91 (2007) 1097.
[15] S.R. Bathe, P.S. Patil, J. Phys. D: Appl. Phys. 40 (2007) 1.
[16] S.R. Bathe, P.S. Patil, Solid State Ionics 179 (2008) 314.
[17] Q. Xiang, G.F. Meng, H.B. Zhao, Y. Zhang, H. Li, W.J. Ma, J.Q. Xu, J. Phys. Chem. C 114 (2010) 2049.
[18] N. Naseri, R. Azimirad, O. Akhavan, A.Z. Moshfegh, Thin Solid Films 518 (2010) 2250.
[19] K.-W. Park, Y.-J. Song, J.-M. Lee, S.-B. Han, Electrochem. Commun. 9 (2007) 2111.
[20] P.S. Patil, S.B. Sadale, An improved spray pyrolysis process for the preparation of good quality thin film semiconducting coatings and apparatus therefor, Indian Patent No. 214163 (2008).
[21] P.R. Selvakannan, S. Mandal, S. Phadtare, A. Gole, R. Pasricha, S.D. Adyanthaya, M. Sastry, J. Colloid Interface Sci. 269 (2004) 97.
[22] K. Boubaker, M. Amlouk, S. Belgacem, J. Alloys Compd. 487 (2009) 286.
[23] P.M. Kadam, N.L. Tarwal, P.S. Shinde, R.S. Patil, H.P. Deshmukh, P.S. Patil, Appl. Phys. A 97 (2009) 323.
[24] T. He, Y. Ma, Y. Cao, W. Yang, J. Yao, J. Electroanal. Chem. 514 (2001) 129.
[25] T. He, Y. Ma, Y. Cao, W. Yang, J. Yao, Phys. Chem. Chem. Phys. 4 (2002) 1637.